ORGANIC LETTERS

2012
Vol. 14, No. 2
548–551

Colorimetric Sensing of Fluoride Ion by New Expanded Calix[4]pyrrole through Anion–π Interaction

Sanjeev P. Mahanta,[†] B. Sathish Kumar,[†] Sambath Baskaran,[‡] Chinnappan Sivasankar,[‡] and Pradeepta K. Panda*,[†]

School of Chemistry, University of Hyderabad, Hyderabad, 500 046, India, and
Department of Chemistry, School of Physical, Chemical and Applied Sciences,
Pondicherry University, Puducherry 605 014, India

pkpsc@uohyd.ernet.in; pradeepta.panda@gmail.com

Received November 26, 2011

ABSTRACT

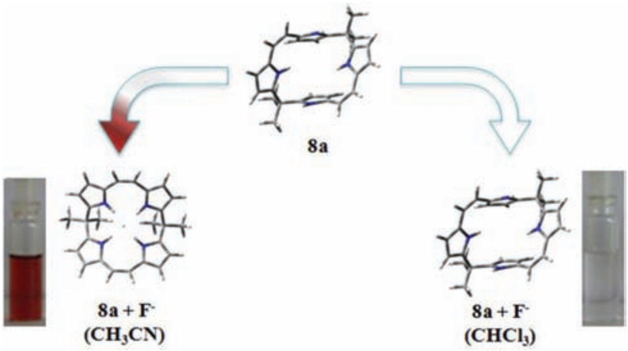

Three new expanded calix[4]pyrroles were synthesized, where the two dialkylldipyrromethane units are linked via C–C double bonds. One of them, calix[2]bispyrrolylethene, colorimetrically senses fluoride ion only, owing to anion–π interaction in polar aprotic solvents.

The selective recognition and sensing of fluoride ion has been the subject of intensive research, motivated by applications in environmental and health sectors especially in dental care[1] and in the treatment of osteoporosis.[2] Owing to its importance, a large number of synthetic receptors containing a H-bond donor motif, with Lewis acidic sites and with an electron-deficient organic π-system, have been designed.[3] In the last two decades, calix[4]pyrroles **1** emerged as an attractive neutral host for anions.[4] In this regard, many transformations and modifications has been carried out on this macrocycle, including

---

[†] University of Hyderabad.

[‡] Pondicherry University.

(1) Matsuo, S.; Kiyomiya, K.; Kurebe, M. *Arch. Toxicol.* **1998**, *72*, 798.

(2) Briancon, D. *Rev. Rheum.* **1997**, *64*, 78.

(3) (a) Takeuchi, M.; Shioya, T.; Swager, T. M. *Angew. Chem., Int. Ed.* **2001**, *40*, 3372. (b) Mizuno, T.; Wei, W.-H.; Eller, L. R.; Sessler, J. L. *J. Am. Chem. Soc.* **2002**, *124*, 1134. (c) Jose, D. A.; Kumar, D. K.; Ganguly, B.; Das, A. *Org. Lett.* **2004**, *6*, 3445. (d) Gomez, D. E.; Fabbrizzi, L.; Licchelli, M. *J. Org. Chem.* **2005**, *70*, 5717. (e) Cametti, M.; Rissanen, K. *Chem. Commun.* **2009**, 2809. (f) Jeong, S.-D.; Nowak-Krol, A.; Kim, Y.; Kim, S.-J.; Gryko, D. T.; Lee, C.-H. *Chem. Commun.* **2010**, *46*, 8737. (g) Wade, C. R.; Broomsgrove, A. E. J.; Aldridge, S.; Gabbai, F. P. *Chem. Rev.* **2010**, *110*, 3958. (h) Sokkolingam, P.; Lee, C.-H. *J. Org. Chem.* **2011**, *76*, 3820.

(4) (a) Baeyer, A. *Ber. Dtsch. Chem. Ges.* **1886**, *19*, 2184. (b) Gale, P. A.; Sessler, J. L; Kral, V.; Lynch, V. *J. Am. Chem. Soc.* **1996**, *118*, 5140.

(5) (a) Gale, P. A.; Sessler, J. L.; Kral, V. *Chem. Commun.* **1998**, 1. (b) Sessler, J. L.; Anzenbacher, P., Jr.; Jursikova, K.; Miyaji, H.; Genge, J. W.; Tvermoes, N. A.; Allen, W. E.; Shiver, J. A. *Pure Appl. Chem.* **1998**, *70*, 2401. (c) Depraetere, S.; Smet, M.; Dehaen, W. *Angew. Chem., Int. Ed.* **1999**, *38*, 3359. (d) Anzenbacher, P., Jr.; Try, A. C.; Miyaji, H.; Jursikova, K.; Lynch, V. M.; Marquez, M.; Sessler, J. L. *J. Am. Chem. Soc.* **2000**, *122*, 10268. (e) Sessler, J. L.; Zimmerman, R. S.; Bucher, C.; Kral, V.; Andriletti, B. *Pure Appl. Chem.* **2001**, *73*, 1041. (f) Gale, P. A.; Anzenbacher, P., Jr.; Sessler, J. L. *Coord. Chem. Rev.* **2001**, *222*, 57. (g) Yoon, D.-W.; Hwang, H.; Lee, C.-H. *Angew. Chem., Int. Ed.* **2002**, *41*, 1757. (h) Custelcean, R.; Delmau, L. H.; Moyer, B. A.; Sessler, J. L.; Cho, W.-S.; Gross, D.; Bates, G. W.; Brooks, S. J.; Light, M. E.; Gale, P. A. *Angew. Chem., Int. Ed.* **2005**, *44*, 2537. (i) Anzenbacher, P., Jr.; Nishiyabu, R.; Palacois, M. A. *Coord. Chem. Rev.* **2006**, *250*, 2929. (j) M. A. Aydogan, A.; Coady, D. J.; Kim, S. K.; Akar, A.; Bielawski, C. W.; Marquez, M.; Sessler, J. L. *Angew. Chem., Int. Ed.* **2008**, *47*, 9648. (k) Namor, A. F. D.; Khalife, R. *J. Phys. Chem. B.* **2008**, *112*, 15766. (l) Ballestera, P.; Gil–Ramírezb, G. *Proc. Natl. Assoc. Sci.* **2009**, *106*, 10455. (m) Panda, P. K.; Mahanta, S. P.; Kumar, B. S. *Chem. Commun.* **2011**, *47*, 4496.

10.1021/ol203165x

meso-substitution(s), β-substitution(s) and core modification.[5] As calix[4]pyrrole mostly binds to smaller halides, to bind larger anions, it was anticipated that larger core size would be more suitable. Toward this, the first expanded calixpyrrole was reported by Sessler and co-workers by the template method;[6] subsequently, higher calix[n]pyrroles were synthesized.[7] Also a new type of expanded calix[4]pyrroles, containing a bigger core size, were made by using spacer units, namely, carbazole **2** and benzene **3** between two 5,5-dimethyldipyrromethane entities.[8a,b] The former macrocycle, namely, calix[4]pyrrole[2]carbazole **2**, although designated as an expanded calix[4]pyrrole entity, but the presence of two additional pyrrole units in the carbazole moieties makes it appear more like a hexapyrrolic macrocycle. Two expanded analogues of **3** were reported by Cafeo et al., where the pyrroles of the dipyrromethane units were connected via meta- or para-phenylenes through additional sp^3-carbon atoms.[8c] It is observed that the expanded calixpyrroles, while displaying enhanced affinity toward larger anions, also display substantial affinity toward fluoride. Among these macrocycles, very few calixpyrrole derivatives display colorimetric sensing and it is ascribed to the presence of chromogenic substituents at the periphery.[9] To our knowledge there is no calixpyrrole-based receptor designed so far to enhance the selectivity toward anions using anion-π interaction strategy.[10]

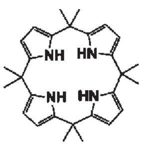

1

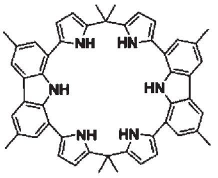

2

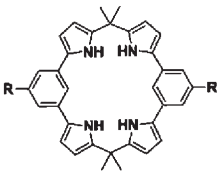

3

Scheme 1

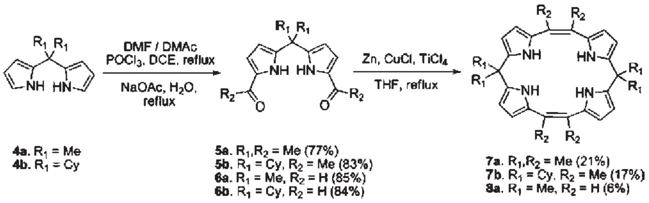

Herein, we have designed new expanded calix[4]pyrroles, where the two dialkyldipyrromethane units are linked via C–C double bonds. Compared to calix[2]bispyrrolylbenzene **3**, these new receptors possess a relatively smaller core size, which in turn is bigger than that of **1**. Further, the presence of two double bonds in the macrocyclic core is expected to influence their anion binding ability through anion–π interactions. For the first time, we report the synthesis of three new expanded calix[4]pyrroles, calix[2]bispyrrolylalkenes, of which calix[2]bispyrrolylethene displays colorimetric sensing of fluoride ion in polar aprotic solvents. These macrocycles are conveniently obtained in two steps from dialkylldipyrromethane **4a**–**b** (Scheme 1). In the first step, **4a**–**b** were separately acylated and formylated to obtain **5a**–**b** (77 and 83%) and **6a**–**b** (85 and 84%), respectively, via the Vielsmeir–Haack method. Subsequent cyclization using McMurry coupling[11] led to the formation of the desired expanded calix[4]pyrroles **7a**–**b** (21 and 17%) and **8a** (only 6%, in spite of many modulations in the reaction conditions) as white solids. McMurry coupling with **6b** did not yield the desired product. This approach, although quite popular in porphyrinoid chemistry, has never been implemented in the synthesis of calixpyrrole derivatives. All of the compounds were characterized by ^{1}H NMR, ^{13}C NMR spectroscopy, mass and elemental analysis. Further, their solid state structures were unequivocally elucidated by single crystal X-ray diffraction method.

Diffraction grade crystals of **7a**, **7b** and **8a** were grown by slow evaporation of dichloromethane (**7a** and **7b**) and ethyl acetate (**8a**) of the respective compounds. All of the compounds adopt 1,3-alternate conformation like **1** (Figure 1). In macrocycle **7a**, two alternate pyrrole units reside in the plane of the meso like C–C double bonds (dihedral angles 3.37 and 4.36°) with their NHs toward the core, while the remaining two pyrrole units adopt almost orthogonal geometry wrt the double bond (dihedral angles 93.78 and 97.54°) and the alternate NHs are directed in opposite direction wrt each other unlike **1**. The presence of cyclohexyl groups at the alternate meso positions create more steric congestion in **7b**, and as a result, the pyrrole units are slightly more distorted compared to **7a** (Supporting Information (SI)). However, owing to the greater steric flexibility, in the case of **8a**, two opposite pyrrole units are found to align slightly away from the cavity (dihedral angles 150.83 and 151.14° wrt the C–C double bonds) with their NHs are directed in opposite direction, whereas the other two pyrrolic entities are oriented toward the core (dihedral angles 11.76 and 13.47° wrt the C–C double bonds) and reside almost in the same plane (Figure 1). The DMSO solvate of **7a**

---

(6) Gale, P. A.; Genge, J. W.; Kral, V.; McKervey, M. A.; Sessler, J. L.; Walker, A. *Tetrahedron Lett.* **1997**, *38*, 8443.

(7) (a) Arumugam, N.; Jang, Y.-S.; Lee, C.-H. *Org. Lett.* **2000**, *2*, 3115. (b) Jang, Y.-S.; Kim, H.–J.; Lee, P.-H.; Lee, C.-H. *Tetrahedron Lett.* **2000**, *41*, 2919. (c) Cafeo, G.; Kohnke, F. H.; Parisi, M. F.; Nascone, R. P.; La Torre, G. L.; Williams, D. J. *Org. Lett.* **2002**, *4*, 2695. (d) Sessler, J. L.; An, D.; Cho, W.-S.; Lynch, V. *Angew. Chem., Int. Ed.* **2003**, *42*, 2278. (e) Bruno, G.; Cafeo, G.; Kohnke, F. H.; Nicolo, F. *Tetrahedron* **2007**, *63*, 10003.

(8) (a) Piatek, P.; Lynch, V. M.; Sessler, J. L. *J. Am. Chem. Soc.* **2004**, *126*, 16073. (b) Sessler, J. L.; An, D.; Cho, W.-S.; Lynch, V.; Marquez, M. *Chem.—Eur. J.* **2005**, *11*, 2001. (c) Cfeo, G.; Kohnke, F. H.; White, A. J. P.; Garozzo, D.; Messina, A. *Chem.—Eur. J.* **2007**, *13*, 649.

(9) (a) Nishiyabu, R.; Anzenbacher, P., Jr. *J. Am. Chem. Soc.* **2005**, *127*, 8270. (b) Nishiyabu, R.; Palacois, M. A.; Dehaen, W.; Anzenbacher, P., Jr. *J. Am. Chem. Soc.* **2006**, *128*, 11496. (c) Yoo, J.; Kim, M.-S.; Hong, S.-J.; Sessler, J. L.; Lee, C.-H. *J. Org. Chem.* **2009**, *74*, 1065.

(10) (a) Gamez, P.; Mooibroek, T. J.; Teat, S. J.; Reedijk, J. *Acc. Chem. Res.* **2007**, *40*, 435. (b) Schottel, B. L.; Chifotides, H. T.; Dunbar, K. R. *Chem. Soc. Rev.* **2008**, *37*, 68. (c) Hay, B. P.; Bryantsev, V. S. *Chem. Commun.* **2008**, 2417. (d) Frontera, A.; Gamesz, P.; Mascal, M.; Mooibroek, T. J.; Reedijk, J. *Angew. Chem., Int. Ed.* **2011**, *50*, 9564. (e) Guha, S.; Saha, S. *J. Am. Chem. Soc.* **2010**, *132*, 17674. (f) Gil-Ramirez, G.; Escudero-Adan, E. C.; Benet-Buchholz, J.; Ballester, P. *Angew. Chem., Int. Ed.* **2008**, *47*, 4114–4118.

(11) Vogel, E.; Kocher, M.; Lex, J.; Ermer, O. *Isr. J. Chem.* **1989**, *29*, 257.

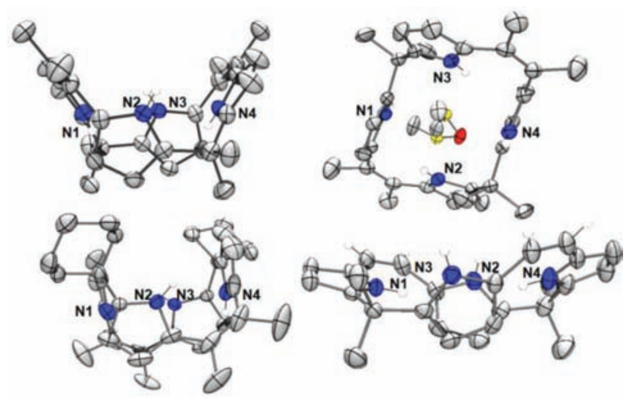

Figure 1. View of the molecular structures. (Top left) **7a** in 1,3-alternate conformation. (Top right) **7a**.DMSO in 1,2-alternate conformation. (Bottom left) **7b** in 1,3-alternate conformation. (Bottom right) **8a** in 1,3-alternate conformation Thermal ellipsoid are scaled to the 35% probability level. All hydrogen atoms bound to carbon atoms are omitted for clarity. Color code: red, O; blue, N; gray, C; yellow, S; white, H.

adopts a slightly distorted 1,2-alternate type conformation (Figure 1).

Preliminary anion binding studies of compound **7a** were carried out in CD_3CN via the ^1H NMR spectroscopic titration method using tetrabutylammonium salts of various anions, namely, F^-, Cl^-, Br^-, I^-, $H_2PO_4^-$, HSO_4^-, ClO_4^-, CH_3COO^-, NO_3^-, CN^- and PF_6^-. The study reveals that **7a** possesses the highest affinity toward fluoride ion, somewhat lesser extent toward acetate ion and little to none toward other anions. Addition of TBAF to **7a** displays a significant downfield shift of the pyrrolic NH from 8.25 to 10.8 ppm with concomitant upfield shift of the β-pyrrolic CH signals; moreover a new sharp peak appears at 7.63 ppm (~0.6 ppm upfield relative to the unbound host NH signal). The intensity of this new signal increases with increased addition of TBAF, whereas its position and sharpness remain unchanged (SI). To reveal the identity of this new peak, we performed D_2O exchange study (SI), which displayed neither exchange nor broadening of this signal even after 24 h, indicating its nonpyrrolic NH nature. ^1H NMR titration of **7a** with acetate ion did not display the new peak. This is indicative of additional binding events in the case of fluoride binding.

Due to the poor solubility of compound **7b** in acetonitrile, its binding studies could not be performed by NMR titration. Further, to understand the fluoride binding events of **7a** and **7b**, we have performed isothermal titration calorimetry (ITC) in acetonitrile which gave K_a values 2.16×10^4 and 3.27×10^4 M^{-1} for **7a** and **7b**, respectively. The ITC profile shows almost eight times more strong binding affinity for **7a** than that measured by NMR (2.65×10^3 M^{-1}), and this discrepancy may be attributed to the presence of another simultaneous event in the host–guest complexation process, which could not be accounted for by NMR titration study. However, screening of **8a** with the previously mentioned anions via ^1H NMR titration in CD_3CN displays a strong colorimetric response for fluoride ion only. A sharp change in color from colorless to dark red resulted immediately with the addition of fluoride ion, which could be clearly observed by the naked eye. Although NMR titration study did not show any significant shift in NH resonance, like **7a**, a new sharp peak appears at 7.58 ppm (1.2 ppm upfield to the unbound host NH signal), again whose position is fixed but intensity increases with fluoride concentration (SI). Macrocycle **8a** did not show any significant change in NH resonance with other anions. The absence of HF_2^- signal in both **7a** and **8a** ruled out the NH deprotonation mechanism. To get further insight into the interaction of fluoride ion with **8a**, the absorption profile of **8a** upon titration with fluoride ion was recorded (Figure 2).

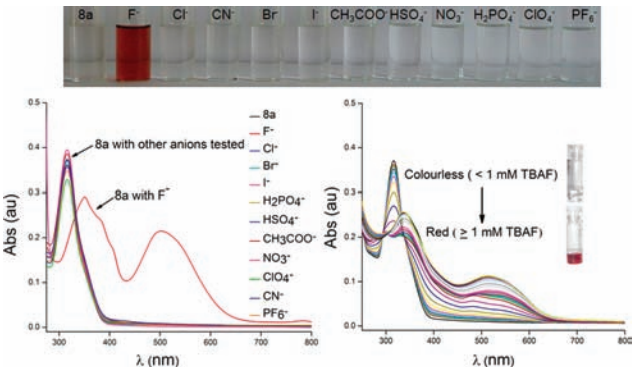

Figure 2. (Top) Colorimetric response of tested anions. (Bottom left) UV–vis spectra of receptor **8a** (20×10^{-6} M in CH_3CN) upon addition of excess tetrabutylammonium salts of tested anions. (Bottom right) Evolution of absorption spectra with gradual addition of $TBAF.3H_2O$ to **8a**.

Upon addition of fluoride ion, two new absorption bands centered at 337 and 515 nm appeared with increasing intensities, which induced the color change to dark red. A detailed inspection revealed that the absorption band centered at 316 nm (free host) decreased gradually up to addition of ~1 mmol fluoride ion with two isosbestic points at 295 and 337 nm. Further addition of TBAF resulted in the red-shift of the spectra with the emergence of new peaks at 337 and 515 nm and hence imparted the resultant colorimetric response. Addition of water to the fluoride complex of **8a** led to a change of color from red to yellow (SI). The above observations (including the disappearence of the isosbestic points) indicate the occurrence of some irreversible process. Further Job's plot analysis confirms the 1:1 stoichiometry for the **8a** and F^- interaction. Competition experiments also confirm the fluoride-induced color change in the presence of other tested anions (SI). Solvent screening displays colorimetric response for **8a** and fluoride ion interaction in polar aprotic solvents like DMSO, DMF, PhCN, THF and EtOAc but not in dichloromethane, chloroform, methanol, isopropanol and *n*-butanol (SI). Electronic paramagnetic resonance study of **7a.F**$^-$ and **8a.F**$^-$ displays a strong signal with *g*-values at 2.0023 and 2.0021, respectively (SI), indicating the presence of an unpaired electron (or anion radical) and thereby confirms the charge transfer nature of the complexes. Unfortunately, we could not obtain any good quality crystal to determine the solid state structure of the host–guest complexes. However, DFT-optimized structures obtained for the **7a.F**$^-$ and **8a.F**$^-$ complexes indicate a more planar type of conformation along with better encapsulation of anion by **8a** than **7a** (Figure 3).

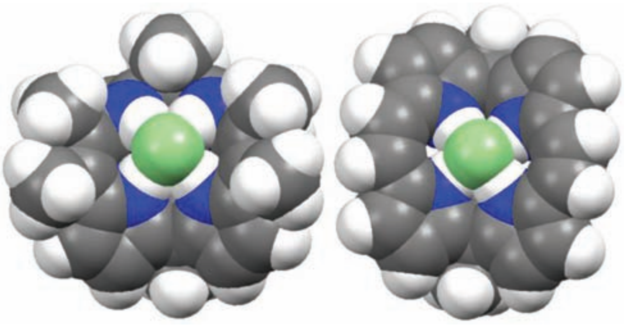

Figure 3. Space filling model of DFT-optimized structure of the fluoride complexes: **7a.F**$^-$ (left) and **8a.F**$^-$ (right). Color code: green, F; blue, N; gray, C; white, H.

Further, HOMO–LUMO energy level determination in the gas phase, chloroform and acetonitrile indicates that while formation of complex raises the energy difference between HOMO and LUMO in **7a** (for example 4.35 to 4.77 eV in acetonitrile (SI)), in the case of **8a** decreases it from 4.02 to 3.71 eV (Figure 4), accompanied by stabilization of both HOMO and LUMO in more polar solvent (viz., acetonitrile) than in the gas phase or less polar solvent (SI) and hence explains its colorimetric response toward fluoride ion. As the LUMO of the macrocycle resides on the C–C double bond, therefore we can conclude that during the complex formation, charge transfer occurs from the fluoride ion to the ethene bonds through anion–π interactions. On the other hand, owing to this charge transfer, the electron density on the fluoride ion is depleted; thereby, it could not interact favorably with the pyrrolic NHs and, hence, probably was the reason why no shift in the NH resonances in ^{1}H NMR of **8a** was observed. The charge transfer process becomes more facile in relatively planar **8a.F**$^-$ complex (hence no shift in NH resonance) than **7a.F**$^-$ (NH resonance shifts from 8.25 to 10.8 ppm); moreover, the presence of electron-donating methyl groups on the bridging double bonds also disfavors the charge transfer from fluoride ion to the host in **7a**.

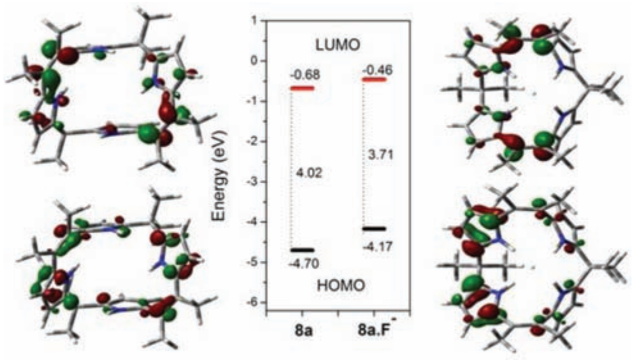

Figure 4. HOMO–LUMO diagrams and energy levels for **8a** and **8a.F**$^-$ in acetonitrile.

In conclusion, we have designed and synthesized three new meso-expanded calix[4]pyrrole receptors following the McMurry strategy for the first time. Among them, calix[2]bispyrrolylethene **8a** displays easy to observe colorimetric sensing of fluoride ion (colorless to dark red) in polar aprotic solvents through anion–π interaction. These macrocycles represent a new class of the smallest expanded calix[4]pyrrole reported so far. Presently, we plan to modulate this system further to enhance its response.

Acknowledgment. This work was supported by DST, India (Project no. SR/S1/IC–20/2007 and SR/FT/CS-055/2008) and CSIR, India (Project no. 01(2449)/10/EMR–II). SPM and BSK thank CSIR for the financial support. We thank Mr. K. Srinivas, Osmania University, Hyderabad for his contribution at the initial stages of the project, during his summer internship under UGC–NRC, School of Chemistry, University of Hyderabad.

Supporting Information Available. Synthetic procedures, full set of characterization data (^{1}H and ^{13}C NMR, LCMS, elemental analysis), fitting of binding curves (ITC and ^{1}H NMR), UV–visible data, EPR, electronic structure calculation, and crystal data for **5a, 6a**, **7a, 7a.DMSO, 7b** and **8a** (CIF). This material is available free of charge via the Internet at http://pubs.acs.org.